ISSN 2072-5981

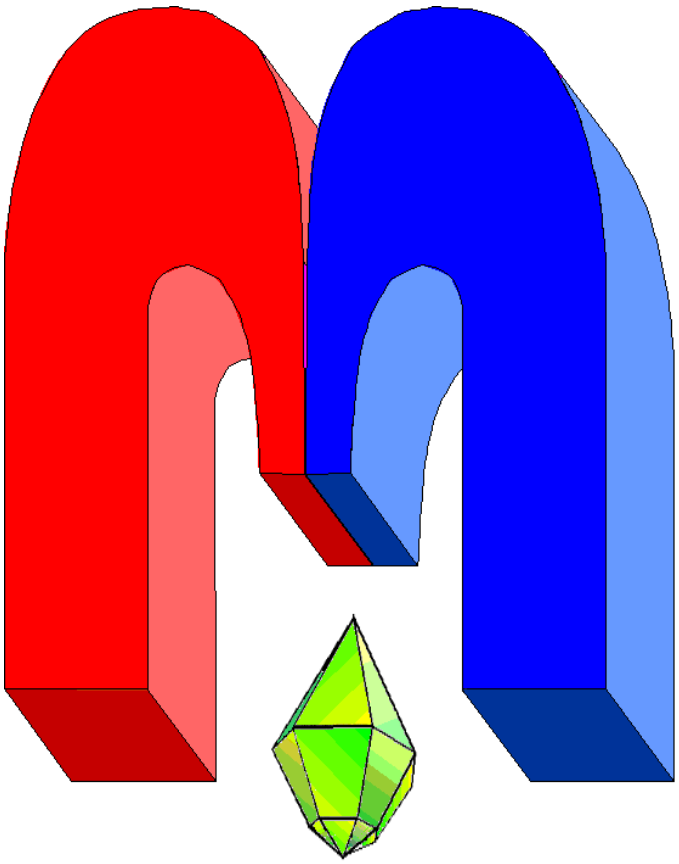

Magnetic Resonance in Solids

Electronic Journal

Volume ***20,***
Issue ***1***
Paper No ***18101,***
1-8 pages
2018

http://mrsej.kpfu.ru
http://mrsej.ksu.ru

Established and published by Kazan University
Sponsored by International Society of Magnetic Resonance (ISMAR)
Registered by Russian Federation Committee on Press, August 2, 1996
First Issue was appeared at July 25, 1997

© Kazan Federal University (KFU)*

"***Magnetic Resonance in Solids. Electronic Journal***" (**MRS*ej***) is a peer-reviewed, all electronic journal, publishing articles which meet the highest standards of scientific quality in the field of basic research of a magnetic resonance in solids and related phenomena.

Indexed and abstracted by
Web of Science (*ESCI*, Clarivate Analytics, from 2015), *Scopus* (Elsevier, from 2012), *RusIndexSC* (*eLibrary*, from 2006), *Google Scholar*, *DOAJ*, *ROAD*, *CyberLeninka* (from 2006), *SCImago Journal & Country Rank*, etc.

Editors-in-Chief

Jean **Jeener** (Universite Libre de Bruxelles, Brussels)

Boris **Kochelaev** (KFU, Kazan)

Raymond **Orbach** (University of California, Riverside)

Executive Editor

Yurii **Proshin** (KFU, Kazan)
mrsej@kpfu.ru

Editors

Vadim **Atsarkin** (Institute of Radio Engineering and Electronics, Moscow)

Yurij **Bunkov** (CNRS, Grenoble)

Mikhail **Eremin** (KFU, Kazan)

David **Fushman** (University of Maryland, College Park)

Hugo **Keller** (University of Zürich, Zürich)

Yoshio **Kitaoka** (Osaka University, Osaka)

Boris **Malkin** (KFU, Kazan)

Alexander **Shengelaya** (Tbilisi State University, Tbilisi)

Jörg **Sichelschmidt** (Max Planck Institute for Chemical Physics of Solids, Dresden)

Haruhiko **Suzuki** (Kanazawa University, Kanazava)

Murat **Tagirov** (KFU, Kazan)

Dmitrii **Tayurskii** (KFU, Kazan)

Valentine **Zhikharev** (KNRTU, Kazan)

This work is licensed under a Creative Commons Attribution-ShareAlike 4.0 International License.

This is an open access journal which means that all content is freely available without charge to the user or his/her institution. This is in accordance with the BOAI definition of open access.

* In Kazan University the Electron Paramagnetic Resonance (EPR) was discovered by Zavoisky E.K. in 1944.

EPR of the V^{4+} ion in single crystals of pyrovanadates β-$Mg_2V_2O_7$, α-$Zn_2V_2O_7$: Spin-Hamiltonian parameters

S.K. Misra [1], S.I. Andronenko [2,*]

[1] Concordia University, 1455 de Maisonneuve Blvd West, Montreal, Quebec, H3G 1M8, Canada

[2] Kazan Federal University, Kremlevskaya 18, Kazan 420008, Russia

**E-mail: Sergey.Andronenko@gmail.com*

(Received November 28, 2017; revised March 19, 2018;
accepted March 19, 2018; published March 30, 2018)

The angular variation of V^{4+} electron paramagnetic resonance (EPR) line positions were recorded in single crystals of β-$Mg_2V_2O_7$ and α-$Zn_2V_2O_7$ at 120 K and 295 K in three mutually perpendicular planes in the temperature range from 120 to 295 K and at some intermediate temperatures. Least-squares fitting was used by diagonalization of the Spin-Hamiltonian (SH) matrix to determine the SH parameters and the orientations of the principal axes of the **g**- and **A**-matrices from the angular variations of the EPR line positions. Although the V^{4+} SH parameters were found to be similar in the two crystals, the orientations of the principal axes of the **g**- and **A**-matrices were not found to be coincident in the two crystals.

PACS: 75.10.Dg, 76.30.-v, 75.20

Keywords: V^{4+} ion, Spin-Hamiltonian parameters, **g**-matrix, **A**-matrix, EPR, pyrovanadates

1. Introduction

Vanadium-mixed oxides (V-Mg-O, V-Zn-O) are important in catalytic processes such as oxidative dehydrogenation of hydrocarbons [1] and selective catalytic reduction of NO by ammonia [2]. The class of vanadia known as vanadates is of great interest now, because these compounds are used in the synthesis of the supported V_2O_7 catalyst [3], insulin-mimetic agents [4] and rechargeable Li batteries [5]. A further point of interest is the thermochromic nature of α-$Zn_2V_2O_7$, which is light yellow in the α phase and changes to red in the β phase [6]. Ioffe *et al.* [7] found that the electrical conductivity of $Mg_2V_2O_7$ and $Zn_2V_2O_7$ pyrovanadates strongly depends on the impurity ions and thermal treatment, which governs the formation of V^{4+} defects. They also obtained qualitative V^{4+} electron paramagnetic resonance (EPR) spectra in Ca, Cd, Mg and Zn pyrovanadates. Crystallochemistry of these compounds was studied experimentally by solid state nuclear magnetic resonance (NMR) [8, 9, 10], and theoretically by using point-monopole approximation and *ab initio* calculations [10, 11]. The Mn^{2+} EPR spectra in single crystals of $Cd_2V_2O_7$ were investigated by Stager [12], whereas the Mn^{2+} EPR spectra in single crystals of $Ca_2V_2O_7$ and $Mg_2V_2O_7$ were investigated by Andronenko *et al.* [13]. Later, the Mn^{2+} EPR spectra in α-$Zn_2V_2O_7$ single crystals were investigated by multifrequency EPR [14]. Recently, the use of nanoparticles of titanium and vanadium oxides as catalysts in Ti-O [15] or V-O [16], has attracted great interest because of its effectiveness in nanostate as compared to that in bulk materials. The doping of catalysts, such as $Mg_2V_2O_7$, with transition metals (Mn, Co, Ni, Fe) also increases its effectiveness [17]. Therefore, investigation of different defects in these compounds, which play a key role in catalysis, is very important to understand the effectiveness of catalytic properties of such oxides.

In this paper we present a precise determination of Spin-Hamiltonian (SH) parameters, specifically the **g**- and **A**-matrices and the orientation of their principal axes of V^{4+} ions in β-$Mg_2V_2O_7$ and α-$Zn_2V_2O_7$ single crystals, and a determination of the position of V^{4+} ions in the crystal structure.

2. Sample preparation and crystal structure

Synthesis

The phase diagrams of ZnO-V_2O_5 and MgO-V_2O_5 systems were investigated to determine the conditions of crystallization of low and high-temperature phases of $Zn_2V_2O_7$ and $Mg_2V_2O_7$ [18, 19]. Single crystals of $Zn_2V_2O_7$ and $Mg_2V_2O_7$ were grown by the spontaneous-crystallization method during slow cooling of the melt with stoichiometric composition using the chemicals V_2O_5 (extreme pure), ZnO (chemically

pure) and $MgCO_3$ (chemically pure). Crystals of $Zn_2V_2O_7$ grew as large rectangular slabs with well-defined (110) cleavage planes. All crystals were twinned, as determined by X-ray diffraction. The growth habits of $Zn_2V_2O_7$ and $Mg_2V_2O_7$ single crystals are shown in Fig. 1 with respect to the orientations of respective laboratory axes *XYZ*. Note, that the authors of [10] investigated NMR spectra of both α and β-$Mg_2V_2O_7$ crystals at room temperature, where β-$Mg_2V_2O_7$ was obtained from α-$Mg_2V_2O_7$ simply with annealing at 850°C during 48 hours, followed by rapid cooling to room temperature. Therefore, the phase transition becomes irreversible and the high-temperature phase is stable at room temperature.

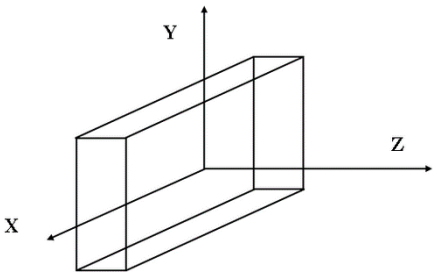

Figure 1. The crystal growth habits of $Mg_2V_2O_7$ and $Zn_2V_2O_7$ crystals in relation to the laboratory axes *XYZ*.

Crystal structure of $Zn_2V_2O_7$

The $Zn_2V_2O_7$ crystal undergoes a fast reversible structural phase transformation at 615°C from the high-temperature thortveitite β-phase (HT phase) with the space group C2/m to the low-temperature α-phase (LT phase) of $Zn_2V_2O_7$, possessing monoclinic symmetry characterized by the space group C2/c with the unit-cell parameters: a = 7.429 Å, b = 8.340 Å, c = 10.098 Å and β = 114.4° and Z = 4 [20]. The main difference between the high (HT) and low (LT) temperature phase structures is that in the former the coordination of Zn ions is six-fold, while in the latter the cations reduce their coordination to five oxygen atoms. In the LT-phase, the ZnO_5 group is a distorted trigonal bipyramid with the longer Zn-O bonds oriented in the axial direction. Vanadium and oxygen ions form V_2O_7 pyrogroups in the structure of α-$Zn_2V_2O_7$. The low-temperature structure contains layers of oxygen atoms stacked perpendicular to the [001] axis, and Zn ions and V-O-V groups lie in octahedrally coordinated sites in alternate layers of oxygen atoms.

Crystal structure of $Mg_2V_2O_7$

The high-temperature β-phase of $Mg_2V_2O_7$ was synthesized at higher temperatures, T > 800°C, above the phase transition between α- and β-phases, at T = 760°C [21]. This phase is stable at room temperature and possesses triclinic space symmetry $P\overline{1}$, with the unit-cell parameters being: a = 13.767 Å, b = 5.414 Å, c = 4.912 Å, α = 81.42°, β = 106.82°, γ = 130.33°, Z = 2 [22]. Only the high-temperature β-phase was investigated here, which remains stable at room temperature. although it is below the phase-transition temperature. The structure of β-$Mg_2V_2O_7$ consists of chains of V_2O_7 groups formed from two VO_4 tetrahedra, which share one common oxygen ion. The adjacent V_2O_7 chains form sheets lying in the (001) plane. They are separated by Mg cations which share oxygen atoms with these sheets.

3. The local structure of V^{5+} ions in $V_2O_7^{4-}$ pyrogroups

The V^{4+} and O^{2-} ions compose $V_2O_7^{4-}$ pyrogroups, which consist of two VO_4 tetrahedra, connected through common O^{2-} ion. This pyrogroup is shown for β-$Mg_2V_2O_7$ in Fig. 2. The point symmetry of the ion in $Mg_2V_2O_7$ is C_i and there are two structurally inequivalent sites for V^{5+} ions in its lattice. In this pyrogroup one V^{5+} ion is 5-fold coordinated and the second V^{5+} ion is 4-fold tetrahedrally coordinated. The corresponding quadrupole coupling parameters (C_Q and η_Q) are different for these two vanadium nuclei, C_Q = 10.1 MHz for the 5-fold coordinated vanadium ions, much larger, than that for the other 4-fold coordinated vanadium ion (C_Q = 4.8 MHz) [9, 10]. There is only one structurally inequivalent site for V^{5+} ions in the $Zn_2V_2O_7$ structure with the point symmetry C_i. The vanadium ion is 4-fold coordinated and the V-O bond lengths as well as the value for C_Q = 3.9 MHz [10] are similar to those in $Mg_2V_2O_7$ for the 4-fold coordinated ion. Therefore, similar the V^{4+}

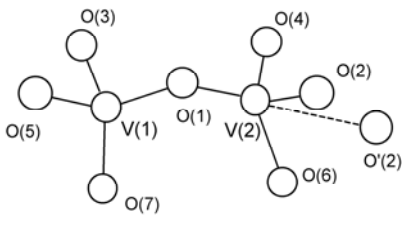

Figure 2. The pyrogroup V_2O_7 in β-$Mg_2V_2O_7$ and α-$Zn_2V_2O_7$ crystals (without O'(2)).

hyperfine (HF) EPR spectra are expected for the V^{4+} ion in these sites in both $Mg_2V_2O_7$ and $Zn_2V_2O_7$ single crystals, and, thus, similar values for V^{4+} hyperfine parameters and the orientations of their principal axes are also expected. The second structurally inequivalent V^{5+} ion, which is situated in distorted tetrahedral configuration associated with the fifth oxygen ion was not observed by EPR in $Mg_2V_2O_7$. Ioffe *et al.* [7] observed another V^{4+} EPR spectrum in $Mg_2V_2O_7$ after annealing it in reduced atmosphere (CO or NH_3 gas at 450°C). They deduced that each hyperfine line of the V^{4+} EPR spectrum split into 8 components by the superhyperfine (SHF) interaction (A_{SHF} = 6 G) with the nearby vanadium nuclei. However, such EPR spectrum was not observed in the presently investigated $Mg_2V_2O_7$ single crystal. The formation of V^{4+} ions ($3d^1$ state) in V-O polyhedra, in which the vanadium ion is in 5-valent state, can be due to the presence of uncontrolled nonmagnetic impurities, or proton (H^+) as an impurity [7]. The EPR spectra for the V^{4+} ion have been observed in many vanadium compounds (CaV_2O_6,V_2O_5) [23, 24]. On the other hand, the V^{4+} EPR spectra were not observed in orthovanadates (YVO_4, $PrVO_4$) [25], implying that the V^{5+} state is stable in 4-fold configuration of VO_4 polyhedra.

4. V^{4+} EPR spectra: determination of SH parameters

Experiment

A Bruker ER-200D SRC EPR X-band spectrometer equipped with nitrogen-flow Bruker variable temperature assembly was used to investigate the EPR spectra in single crystals of β-$Mg_2V_2O_7$ and α-$Zn_2V_2O_7$. Usual setting of EPR spectrometer: modulation field is 1-5 G / 100 kHz and microwave power is 20 Db (max output power is 200 mW). The EPR spectra of the V^{4+} ions were recorded at X-band (9.6 GHz) in the temperature range 120-300 K. Only one magnetically inequivalent V^{4+} ion was observed in the two crystals in the temperature range accessible in the present experiment. Detailed angular variations of V^{4+} X-band EPR line positions were recorded at 120 K and 290 K in three mutually perpendicular planes in the two single crystals. They are shown in Figs. 3a,b,c and 3d,e,f respectively. The angular variations of V^{4+} X-band EPR spectra recorded at 290 K in tree mutually perpendicular planes in β-$Mg_2V_2O_7$ single crystal are similar to those shown in Figs. 3 for α-$Zn_2V_2O_7$ single crystal, and not shown here. In each plane, the magnetic field orientation was varied at 5° intervals. The orientation of the principal axes corresponding to the largest principal *g*-value, i.e. the direction of the Zeeman field for which the positions of the lines are at their minimum, in this plane was chosen to be the magnetic *Z'*-axis, which was found to be approximately perpendicular to largest flat surface of the crystal. The *Z*-axis and *Z'*-axis are not coincident. For EPR measurements in the laboratory *ZY* and *XY* planes the specimen was oriented in such a way that it could be rotated about the *X* and *Z*-axes, keeping the external static magnetic field fixed.

Spin-Hamiltonian parameters

The spin-Hamiltonian of the V^{4+} ion, describing the interaction of its magnetic moment with the external magnetic field **B**, and the hyperfine (HF) interaction with its own ^{51}V nucleus, is written in following form [26]:

$$H = \mu_B \mathbf{BgS} + \mathbf{SAI}, \tag{1}$$

where μ_B is the Bohr magneton, S = ½ is electronic spin of the V^{4+} ion, and **g** is the **g**-matrix, [26]. The ^{51}V nucleus (99.76% natural abundance) has the nuclear spin I = 7/2 (g_n = 1.468); thus, each line splits into eight HF lines at X-band. In Eq. (1) **A** is HF interaction matrix; the principal axes of the **g** and **A** matrices are, in general, not coincident with each other for low (monoclinic and triclinic) symmetries. A rigorous least-squares fitting of EPR line positions in three mutually perpendicular planes to the SH parameters enabled determination of the orientations of the principal axes of the **g** and **A** matrices [27, 28]. Two fitting programs were used here in the evaluation of the SH parameters, one for fitting the principal values and their orientations of the **g**-matrix and the second one for fitting the principal values of the **A** matrix. The results are listed in Tables 1-6.

The orientations of the principal axes of the **g**-matrix are denoted as *Z′X′Y′*, whereas the principal axes of the **A**-matrix are denoted as *Z″X″Y″*. The principal values of g are dimensionless, while those of **A** are expressed in GHz. The indicated errors are estimated by the use of a statistical method as outlined

by Misra and Subramanian [29]. The direction cosines of the principal axes of the **g**-matrix (*X′*, *Y′*, *Z′*) are given with respect to the laboratory, *XYZ*-axes defined in section 2, whereas those of the **A**-matrix (*X″Y″Z″*) are expressed relative to (*X′Y′Z′*).

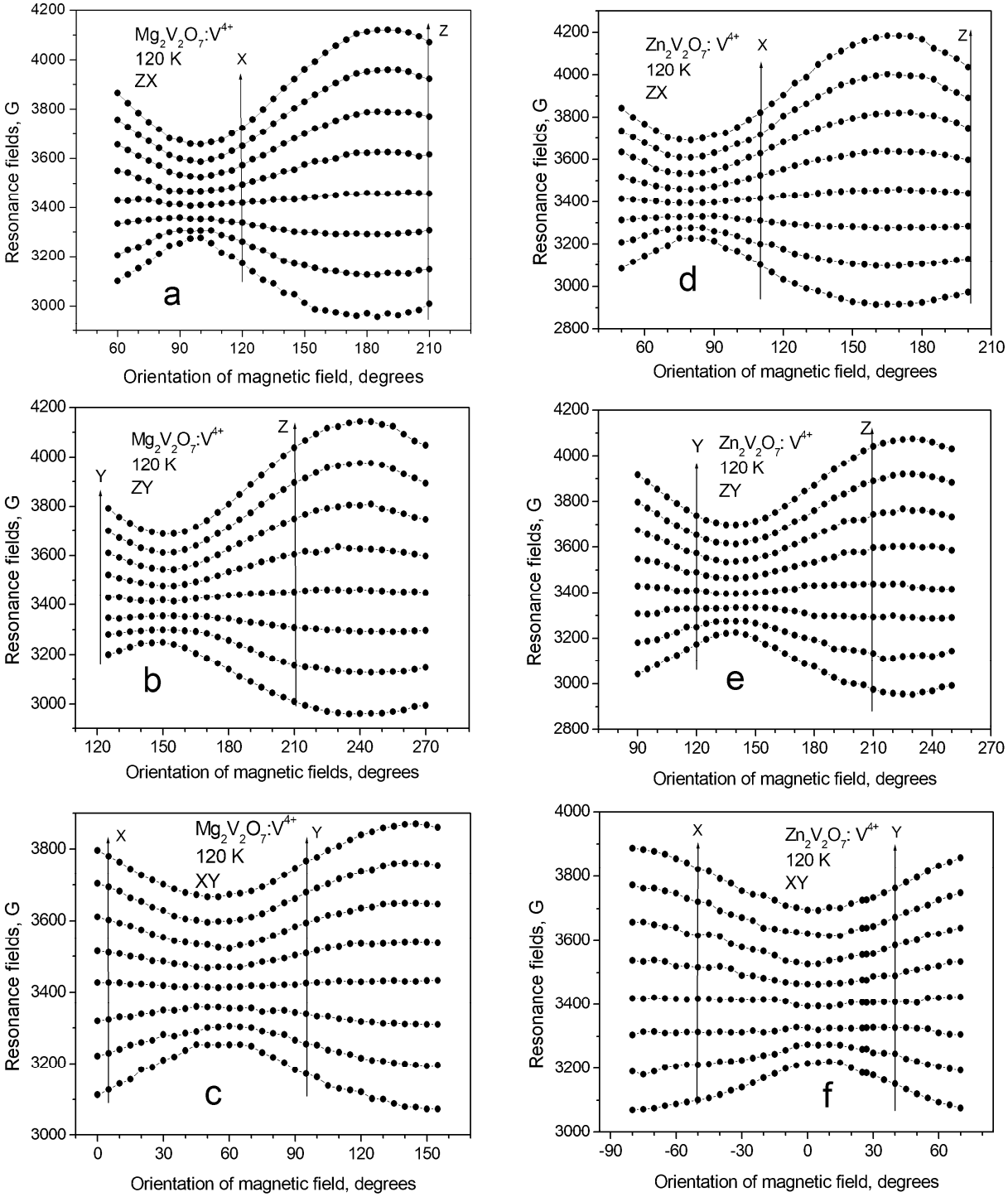

Figure 3. Angular variations of the V^{4+} EPR spectra at 120 K in single crystals of $Mg_2V_2O_7$ and $Zn_2V_2O_7$, respectively, in three mutually perpendicular planes in the laboratory coordinate system; panels (a) and (d) correspond to *ZX*; (b) and (e) correspond to *ZY*; (c) and (f) correspond to *XY*.

Temperature dependence and unresolved SHF splitting

The EPR spectra in the temperature range from 120 to 295 K for the specific orientations of the magnetic fields in β-$Mg_2V_2O_7$ and α-$Zn_2V_2O_7$ are shown in Figs. 4a and 4b, respectively. The EPR spectra were recorded for $Mg_2V_2O_7$ for the orientations of the external magnetic field in the *ZY* plane, whereas those

for $Zn_2V_2O_7$ for the orientations of the external magnetic field in the *ZX* plane. There was observed no significant temperature dependence of the EPR linewidth for V^{4+} ions in the temperature range 120-290 K. The average V^{4+} EPR linewidth is rather large, about 30-35 G. It is due to the superhyperfine (SHF) interaction of spin of the V^{4+} ion with nearest V nucleus (I = 7/2), which splits each HF line into eight unresolved SHF lines. If the individual EPR linewidth is larger than 5 G, then unresolved SHF structure will appear. The SHF interaction constant can be estimated to be 5-6 G, which is reasonable, similar to that observed by Ioffe *et al.* [7] in pyrovanadates for the "second" EPR V^{4+} center (A_{SHF} = 6 G).

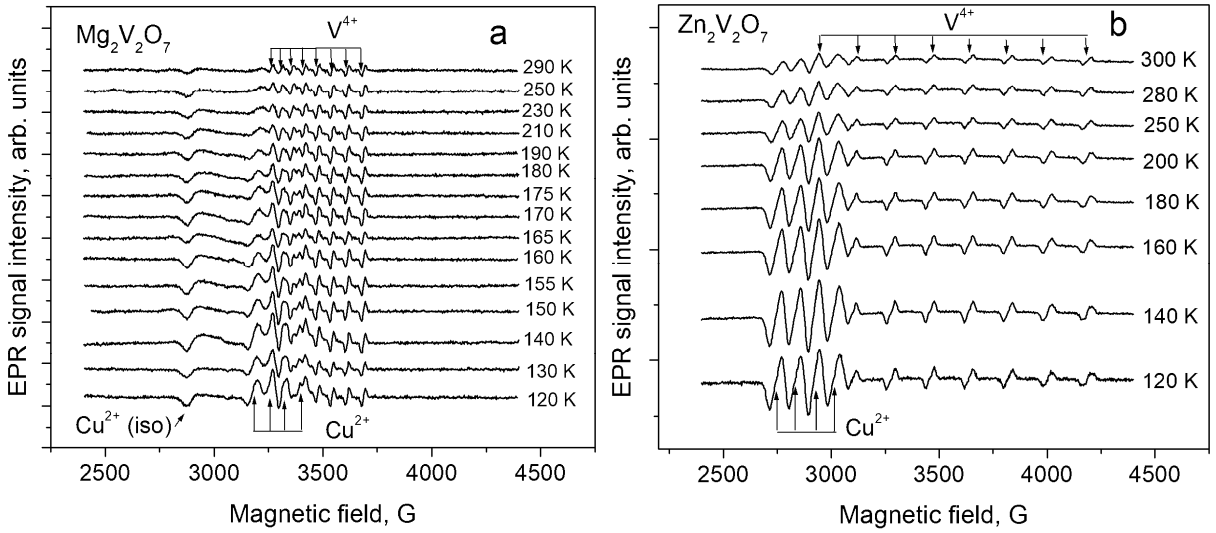

Figure 4. The EPR spectra in $Mg_2V_2O_7$ and $Zn_2V_2O_7$ single crystals at various temperatures for the particular orientation of the external magnetic field. Fig. 4a: β = 150°, *ZY* plane (as shown in Fig. 3b), minimum HF splitting and Fig. 4b: α = 170°, *ZX* plane (as shown in Fig. 3d), maximum HF splitting, respectively. The EPR lines for Cu^{2+}, also present as impurity, are seen at lower magnetic fields.

Table 1. The principal values of the **g**-matrices of the V^{4+} ions in single crystals of β-$Mg_2V_2O_7$ and α-$Zn_2V_2O_7$ at 120 K and 290 K. The numbers of V^{4+} EPR lines fitted to EPR line positions at 120 and 290 K under consideration in β-$Mg_2V_2O_7$ are 808 and 744, and those in α-$Zn_2V_2O_7$ are 768 and 768. SMD (GHz^2) ≡ $\Sigma_i (\Delta E_i/h - \nu_i)^2$, where ($\Delta E_i$ is the calculated energy difference in GHz between the levels participating in resonance for the i^{th} line position; ν_i is the corresponding klystron frequency in GHz, h is Planck's constant; RMSL(GHz) = (SMD/n)$^{1/2}$ is average mean-square deviation of energy level difference from klystron frequency.

	Temperature (K)	g_Z	g_X	g_Y	n	RMSL (GHz)
$Mg_2V_2O_7$	295	1.930 ± 0.001	1.977 ± 0.001	1.996 ± 0.001	744	0.006
	120	1.932 ± 0.001	1.969 ± 0.001	2.002 ± 0.001	808	0.011
$Zn_2V_2O_7$	295	1.928 ± 0.001	1.969 ± 0.001	2.013 ± 0.001	768	0.016
	120	1.932 ± 0.001	1.976 ± 0.001	2.011 ± 0.001	768	0.014

Table 2. The principal values of the **A**-matrices of the V^{4+} ions in single crystals of β-$Mg_2V_2O_7$ and α-$Zn_2V_2O_7$ at 120 K and 295 K.

	Temperature (K)	A_Z(GHz)	A_X(GHz)	A_Y(GHz)	n	RMSL (GHz)
$Mg_2V_2O_7$	295	0.480 ± 0.005	0.185 ± 0.005	0.147 ± 0.005	744	0.058
	120	0.490 ± 0.005	0.170 ± 0.005	0.156 ± 0.005	808	0.055
$Zn_2V_2O_7$	295	0.504 ± 0.005	0.189 ± 0.005	0.170 ± 0.005	768	0.083
	120	0.500 ± 0.005	0.194 ± 0.005	0.179 ± 0.005	768	0.060

Table 3. The principal values and direction cosines of the principal axes of the **g**-matrices for the V^{4+} ions in single crystals of β-$Mg_2V_2O_7$ at 120 K and 295 K.

Temp. (K)	g_Z, g_X, g_Y	Direction cosines		
		Z/Z'	*X/X'*	*Y/Y'*
295	$g_Z = 1.930$	0.924	0.210	0.318
	$g_X = 1.977$	–0.105	–0.660	0.744
	$g_Y = 1.996$	–0.366	–0.721	0.588
120	$g_Z = 1.932$	0.927	–0.083	–0.365
	$g_X = 1.969$	0.215	–0.680	0.701
	$g_Y = 2.002$	0.306	0.729	0.612

Table 4. The principal values and direction cosines of the principal axes of the **A**-matrices for the V^{4+} ion in a single crystal of β-$Mg_2V_2O_7$ at 120 K and 295 K.

Temp. (K)	A_Z, A_X, A_Y	Direction cosines		
		Z/Z'	*X/X'*	*Y/Y'*
295	$A_Z = 0.480$	0.863	0.433	–0.260
	$A_X = 0.185$	–0.424	0.901	0.094
	$A_Y = 0.147$	0.275	0.029	0.961
120	$A_Z = 0.490$	0.891	–0.359	0.278
	$A_X = 0.170$	0.241	0.893	0.381
	$A_Y = 0.156$	–0.385	–0.272	0.882

Table 5. The principal values and direction cosines of the principal axes of the **g**-matrices for the V^{4+} ion in a single crystal of α-$Zn_2V_2O_7$ at 120 K and 295 K.

Temp. (K)	g_Z, g_X, g_Y	Direction cosines		
		Z'/Z"	*X'/X"*	*Y'/Y"*
295	$g_Z = 1.928$	0.780	0.373	–0.502
	$g_X = 1.969$	0.623	–0.537	0.569
	$g_Y = 2.013$	0.057	0.757	0.651
120	$g_Z = 1.932$	0.846	0.294	–0.444
	$g_X = 1.976$	0.528	–0.570	0.629
	$g_Y = 2.011$	0.068	0.767	0.638

Table 6. The principal values and direction cosines of the principal axes of the **A**-matrices for the V^{4+} ion in a single crystal of α-$Zn_2V_2O_7$ at 120 K and 295 K.

Temp. (K)	A_Z, A_X, A_Y	Direction cosines		
		Z'/Z'	*X'/X"*	*Y'/Y"*
295	$A_Z = 0.504$	0.944	–0.057	0.324
	$A_X = 0.189$	–0.269	–0.434	0.860
	$A_Y = 0.170$	–0.189	–0.899	0.394
120	$A_Z = 0.500$	0.966	–0.031	0.258
	$A_X = 0.194$	–0.086	0.899	0.430
	$A_Y = 0.180$	–0.246	0.437	0.865

5. Coordination of the V^{4+} ion ($3d^1$) in VO_4 polyhedra

The point symmetry of the vanadium ion is C_i in $Mg_2V_2O_7$ for the two magnetically inequivalent sites for V^{5+} ions. The V^{5+} ion is situated in the first VO_4 tetrahedron, V(1) is 4-fold tetrahedrally coordinated, with the V(1) – O(n) bonding lengths varying from 1.682 to 1.784 Å. The V^{5+} ion is situated in the second VO_4 tetrahedron, V(2), with the bonding lengths from 1.629 to 1.817 Å [22]. It is distorted with the additional bonding to the fifth oxygen ion (V(2) – O(5), with the bonding length being 2.44 Å [22]). In α-$Zn_2V_2O_7$, the V^{5+} ion possesses C_i point symmetry. There is only one magnetically inequivalent site for the V^{4+} ion, which occupies a V^{5+} site. This V^{4+} ion, situated at a regular V^{5+} site, is 4-fold tetrahedrally coordinated with the bonding lengths varying from 1.658-1.775 Å [20]. The $3d^1$ configuration of the V^{4+} ion is split in cubic crystal field into a Γ_3 doublet and a Γ_5 triplet [26]. In tetrahedral coordination, the Γ_3 doublet lies lower, representing the ground state [26]. The spin-orbit coupling constant λ is positive for tetrahedral coordination. Further, the Γ_3 doublet is split into a Γ_1^t singlet (wavefunction $|3z^2 - r^2\rangle$) and Γ_3^t singlet (wavefunction $|x^2 - y^2\rangle$) [26]. Unfortunately, the V^{4+} ion possesses a very low symmetry in β-$Mg_2V_2O_7$ and α-$Zn_2V_2O_7$ crystals, thus, it is not possible to

determine its actual ground state wavefunction from the available experimental data. The principal values of the **g**- and **A**-matrices, obtained here for $Mg_2V_2O_7$ and $Zn_2V_2O_7$ are close to those obtained by Ioffe *et al.* [23] for the V^{4+} ion in $Ca_2V_2O_7$ single crystal, which is isostructural to the triclinic $Mg_2V_2O_7$ (with the parameters $g_Z = 1.948$; $g_X = 1.966$; $g_Y = 1.975$; and $A_Z = 0.475$ GHz; $A_X = 0.150$ GHz; $A_Y = 0.138$ GHz), from which they determined the ground state function of the V^{4+} ion to be $|x^2 - y^2\rangle$. They did not determine the orientations of the principal axes of **g**- and **A**-matrices.

The principal values of the **g**- and **A**-matrices are very similar to each other for the V^{4+} ions in $Mg_2V_2O_7$ and $Zn_2V_2O_7$ single crystals. This is because the V(1) ion in $Mg_2V_2O_7$ is 4-fold coordinated and the average bonding length V(1) – O(n) is 1.730 Å, very close to the average bonding length V – O(n) in $Zn_2V_2O_7$, which is 1.716 Å. The values of **g**- and **A**-matrices depend strongly on overlap of the wave functions of the V^{4+} ions and neighboring oxygen ligands. Therefore, one can deduce that the V^{4+} ion occupies the V(1) crystallographic position in $Mg_2V_2O_7$ single crystals. This conclusion was supported by NMR of ^{51}V nucleus in β-$Mg_2V_2O_7$ and α-$Zn_2V_2O_7$ [9, 10]. The values for quadrupole coupling parameters are: $C_Q = 4.8$ MHz for V(1) and $C_Q = 10.1$ for V(2) in β-$Mg_2V_2O_7$ and $C_Q = 3.68$ MHz for α-$Zn_2V_2O_7$ [9, 10]. Both the V(1) ion in β-$Mg_2V_2O_7$ and the V ion in α-$Zn_2V_2O_7$ are 4-fold coordinated and possess similar values of C_Q. This result was proved also by theoretical calculations of C_Q [11]. Therefore, the environments of V(1) in β-$Mg_2V_2O_7$ and V ions in α-$Zn_2V_2O_7$ are similar and the V^{4+} ions, which occupy these sites, expect to have similar SH parameters. The orientations of the principal axes of the **g**-matrices *Z'*, *X'*, *Y'* of the V^{4+} ions relative to the crystal faces are also similar in the two crystals, with the *Z'*-axis being perpendicular to the (110) cleavage plane (*XY* plane, see Fig. 1) for α-$Zn_2V_2O_7$, which implies that the cleavage plane of $Mg_2V_2O_7$ is also the (110) plane.

The V^{4+} EPR spectra in several vanadium compounds have been observed over a very large temperature range up to room temperature. For its temperature stability the O_3 - V^{4+}- O – V^{5+} - O_3 pyrogroup should be charge-compensated with the positive charge being in the vicinity. Ioffe *et al.* [7] indeed showed that the charge compensation is due to proton (H^+) being in an interstitial position to render the V^{4+} ion stable.

6. Conclusions

The main conclusions of the V^{4+} EPR investigations in β-$Mg_2V_2O_7$ and α-$Zn_2V_2O_7$ single crystals are as follows:

(i) The principal values of the **g** and **A** matrices of the V^{4+} ion and their orientations relative to the crystal faces system have been determined in these crystals.

(ii) The SH parameters of the V^{4+} ion in β-$Mg_2V_2O_7$ and α-$Zn_2V_2O_7$ single crystals are found to be similar because the V^{4+} ions occupy similar tetrahedrally coordinated crystallographic sites in them.

(iii) The principal axes of the **g**-matrix are not coincident with those of the **A**-matrix because of the low point symmetry C_i.

Acknowledgments

This work is supported by Natural Sciences and Engineering Research Council of Canada (NSERC) (SKM). SIA is grateful for partial support in the frame of research project allocated to Kazan Federal University, Russia for the state assignment in the sphere of scientific activities (#3.2166.2017/4.6).

References

1. Blasco T, Nieto J.M.L. *Appl. Catal.* **A157**, 117 (1997)
2. Busca G., Lietti L., Ramis G., Betti F. *Appl. Catal. B* **18**, 1 (1998)
3. Blasco T., Nieto J.M.L., Dejoz A., Vazquez M.I. *J. Catal.* **157**, 271 (1995)
4. Thompson K.H., McNeill J.H., Orvig C. *Chem. Rev.* **99**, 2561 (1999)

5. Pistoia G., Wang G., Zane D. *Sol. St. Ionic* **76**, 285 (1995)
6. Brown J.J., Hummel F.A. *Trans. Brit. Ceram. Soc.* **64**, 419 (1965)
7. Ioffe V.A., Grunin V.S., Zonn Z.N., Ivanov S.E., Yanchevskaya I.S. *Inorganic Materials* (*engl. trans. of Izv. Akad. Nauk SSSR*, *Neorg. Mater.*) **13**, 1484 (1977)
8. Ioffe V.A., Moskalev V.V., Dmitrieva L.V., Ivanov S.E., Zonn Z.N. *Sov. Phys. Solid. State.* **17**, 2043 (1976)
9. Andronenko S.I., Dmitrieva L.V., Molodchenko N.G., Moskalev V.V., Zonn Z.N. *Sov. Phys. Solid. State.* **21**, 535 (1979)
10. Nielsen V.G., Jakobsen H.J., Skibsted J. *J. Phys. Chem. B* **105**, 420 (2001)
11. Lo A.Y.H., Hanna J.V., Schurko R.W. *Appl. Magn. Reson.***32**, 691 (2007)
12. Stager C.V. *Can. J. Phys.* **46**, 807 (1968)
13. Ioffe V.A., Andronenko S.I., Zonn Z.N. *in Magnetic Resonance and Related Phenomena: Proceedings of the 20th Congress AMPERE*, *Tallinn*, 1978, Berlin, p. 305 (1979)
14. Misra S.K., Andronenko S.I. Earle K.A., Freed J.H. *Appl. Magn. Reson.* **21**, 549 (2001)
15. Misra S.K., Andronenko S.I., Tipikin D., Freed J.H., Somani V., Prakash O. *J. Magn. Magn. Mater.* **401**, 495 (2016)
16. Guimond S., Abu Haija M., Kaya S., Lu J., Weissenrieder J. Shaikhutdinov S., Kuhlenbeck H., Freund H.-J., Döbler J., Sauer J. *Top. Catal.* **38**, 117 (2006)
17. Xia Q., Obana Y., Nishiguchi H., Ito M., Ishihara T., Takita Y. *J. Jpn. Petrol. Inst.* **46**, 87 (2003)
18. Kurzawa M., Rychlowska-Himmel I., Bosacka M., Blonska-Tabero A. *J. Therm. Anal. Calorim.* **64**, 1113 (2001)
19. Clark G.M., Morley R. *J. Solid State Chem.* **16**, 429 (1976)
20. Gopal R., Calvo C. *Can. J. Chem.* **51**, 1004 (1973)
21. Krasnenko T.I., Vasyutinskaya E.F., Zolotukhina L.V., Dobrynin B.E., Slobodin B.V. *Russ. J. Inorg. Chem.* **46**, 733 (2001)
22. Gopal R., Calvo C. *Acta Cryst.* **B30**, 2491 (1974)
23. Ioffe V.A., Grunin V.S., Patrina I.B. Yanchevskaya I.S. *in Magnetic Resonance and Related Phenomena: Proceedings of the 18th Congress AMPERE*, *Nottingham 1974*, North-Holland, Amsterdam, p.123 (1975)
24. Grunin V.S., Patrina I.B., Andronenko S.I., Zonn Z.N. *Sov. Phys. Solid. State* **23**, 1274 (1981)
25. Andronenko S.I., Ioffe V.A., Udalov Yu.P. *Sov. Phys. Solid State* **23**, 1478 (1981)
26. Abragam A., Bleaney B. *Electron Paramagnetic Resonance of Transition Ions*, Clarendon Press, Oxford (1970)
27. Misra S.K. *J. Magn. Reson.* **23**, 403 (1976)
28. Misra S.K. *Physica B* **151**, 433 (1988)
29. Misra S.K., Subramanian S. *J. Phys. C.: Sol. St. Phys*. **15**, 7199 (1982)